Preliminaries to analysis of heterogeneous materials using meshless methods

Bachelor Thesis

by

Jaroslav Vondřejc

born on the 27th of February 1983 in Opočno

May 2008

Supervisor:
Ing. Jan Zeman Ph.D.

Czech Technical University in Prague
Faculty of Civil Engineering
Department of Mechanics

Contents

List of Figures

List of Tables

Abstract

Title: Preliminaries to analysis of heterogeneous materials using meshless methods

The aim of thesis: In the field of engineering design many complex problems are solved with numerical techniques. Beside Finite Element Methods that is a very powerfull tool and mesh-based methods in general, the meshless methods can be used. This project is based on onalysing two meshless methods in one dimensional space. The first method is called the Boundary Point Method (BPM) that uses function approximation with basis function. The second one is named the Fast Fourier Transform (FFT) Based Method. In the contrary to previous method, it uses iteration algorithm to obtain solution.

Method: The algorithm of each method is implemented into the software `MATLAB` and subsequently the parameters of the methods are analysed. The goal of methods analysing is to explore the algorithm behaviour applied to one dimensional rod and consequently find the optimal values of parameters for best convergence.

Results: Boundary Point Method mostly depends on ability to approximate demanded deformation with basis function $\varphi(x)$. The parameters of this method are the number of discretizing nodes N and the parameter H determining the "hat" shape of basis function $\varphi(x)$. While the increasing number of discretizing nodes N causes better approximation, the parameter H is rather complicated. Nevertheless the optimal value for observed function was found in interval $\langle 0.4, 3.3\rangle$. The problem of function approximation and consequently BPM is Gibb's effect.

Fast Fourier Transform Based Method is determined, similarly as in previous case, with the number of discretizing nodes N. The second parameter is E_{ref} that is usually put into the relation with E_0 and E_1 stiffnesses. The number of iteration does not depened on the value N. The increasing number of discretizing nodes N just better specifies deformation along the rod. For the ratio $\frac{E_0+E_1}{E_0}$ greater than approximately 5, the optimal value of E_{ref} is close to value $\left(E_0 + \frac{E_1}{2}\right)$.

Key words: Heterogeneous materials, Boundary Point method, discretization, approximation, Fast Fourier Transform

Chapter 1

Theory

1.1 Introduction

In the field of engineering design we come across many complex problems, the mathematical formulation of which is tedious and usually not possible by analytical methods. At such instants we resort to the use of numerical techniques. Here lies the importance of Finite Element Method (FEM), which is a very powerful tool for getting the numerical solution of a wide range of engineering problems. The basic concept is that a body or structure may be divided into smaller elements of finite dimensions called as Finite Elements [1].

Contrary to FEM and mesh-based methods in general there exist situations where some of the meshless methods is convenient to use. This project is based on analysing two meshless methods in one dimension and this Chapter provides theoretical information about them.

The first method described in Section 1.2 is based on discretisation using the Gauss approximation functions. The method itself produces the Toeplitz structured matrices due to the regular discretisation grid and even approximation functions. Hence the systems can be advantageously solved using iterative solvers based on Fast Fourier Transform (FFT) technique. On the other hand there are problems with setting parameters in order to avoid less efficiency or even divergence.

The second method described in Section 1.3 is based on iteration algorithm at the regular discretisation grid of periodically repeating medium.

In the next Chapter 2 the algorithms used for analysing those methods are provided. Finally the last Chapter 3 discuss the results obtained from analysing the both methods.

1.2 Boundary Point Method

The Boundary Point Method (BPM) is a quite new numerical approach designed for a solution of various problems of applied mathematics and physics. It was introduced by Russian mathematican Maz'ya in the 90's of the last century. Contrary to a very popular Finite Element Method discretising differential equations, the BPM is based on the discretisation of integral equations.

This Section provides various information about this method on the simplest one-dimensional case. The first part at Section 1.2.1 starts with problem discretization, the second part at Section 1.2.2 covers function approximation that is used in the BPM. That

approximation is used in Section 1.2.3 where the finalization of BPM is provided. The information about the theory of BPM is drawn up from Novák [2].

1.2.1 Problem Discretization

This Section provides theoretical introduction to analyzing one dimensional rod with heterogeneities. It is necessary to note that the rod has unit cross-section hence it is not included in the formulas. In general the solution of deformation consist of setting equilibrium equation at the rod:

$$\frac{d}{dx}\left(E(x)\frac{du(x)}{dx}\right) + g(x) = 0 \tag{1.1}$$

where $E(x)$ is Young's modulus and $g(x)$ is load function causing $u(x)$ displacement.

In this method the infinite one dimensional rod with heterogeneities is considered. The rod is loaded at infinity with deformation ε_0. The material data is described with stiffness function $E(x)$, which is separated into two components:

$$E(x) = E_0 + E_1(x) \tag{1.2}$$

where E_0 is Young's modulus of material of matrix, $E_1(x)$ is its complement to real stiffness. The BPM method assumes that $E_1(x)$ function has a nonzero values only on a finite interval $\langle a, b\rangle$. identically equal to zero. For the use of the method, the deformation $\frac{du(x)}{dx} = \varepsilon(x)$ is separated into two components as stated below:

$$\varepsilon(x) = \varepsilon_0 + \varepsilon_1(x) \tag{1.3}$$

where $\varepsilon_1(x)$ deformation is complement to real deformation.

Hence the general problem, Equation (1.1), can be rewritten into the following form:

$$\frac{d}{dx}\Big[\Big(E_0 + E_1(x)\Big)\Big(\varepsilon_0 + \varepsilon_1(x)\Big)\Big] = 0 \tag{1.4}$$

$$\frac{d}{dx}\Big(E_0\varepsilon_0 + E_0\varepsilon_1(x) + E_1(x)\varepsilon_0 + E_1(x)\varepsilon_1(x)\Big) = 0 \tag{1.5}$$

After several algebraic emendations and using $\frac{d}{dx}(E_0\varepsilon_0) = 0$, it follows:

$$\frac{d}{dx}\Big(E_0\varepsilon_1(x)\Big) = -\frac{d}{dx}\Big[E_1(x)\varepsilon_0 + E_1(x)\varepsilon_1(x)\Big] \tag{1.6}$$

The left side of Equation (1.6) can be interpret as homogeneous rod with stiffness E_0 and deformation $\varepsilon_1(x)$. Hence, the right side of the Equation (1.6) can be interpret as generalized load $f(x)$ causing that $\varepsilon_1(x)$ deformation:

$$f(x) = -\frac{d}{dx}\Big(E_1(x)\varepsilon(x)\Big) \tag{1.7}$$

Now we can take a look at displacement using Green function. It is defined as follows:

$$u_1(x) = \int_{-\infty}^{\infty} G(x,y)f(y)dy \tag{1.8}$$

The derivation of Equation (1.8) and using expression for $f(x)$ from Equation (1.7) leads to:

$$\frac{du_1(x)}{dx} = \varepsilon_1(x) = -\int_{-\infty}^{\infty} \frac{\partial G(x,y)}{\partial x} \frac{d}{dy}\Big(E_1(y)\varepsilon(y)\Big)dy \tag{1.9}$$

Integration by parts leads to:

$$\varepsilon_1(x) \overset{P.P.}{=} \int_{-\infty}^{\infty} \frac{\partial^2 G(x,y)}{\partial x \partial y} E_1(y)\varepsilon(y)dy - \frac{\partial G(x,y)}{\partial x} E_1(y)\varepsilon(y)\Big|_{-\infty}^{\infty} \tag{1.10}$$

The second term in Equation (1.10) is equal to zero as $\lim_{x\to\pm\infty} E_1(y) = 0$. Noting that the variables x and y in function $\frac{\partial G(x,y)}{\partial x \partial y}$ depends just on their difference it can be simplified as follows $\frac{\partial G(x,y)}{\partial x \partial y} = K^{\infty}(x-y)$. Hence, Equation (1.10) leads to:

$$\varepsilon_1(x) = \int_{-\infty}^{\infty} K^{\infty}(x-y)E_1(y)\varepsilon(y)dy \tag{1.11}$$

To solve the last equation it is necessary to know something about the function $K^{\infty}(x-y)$. It could be proved using Fourier Transform that equals to:

$$K^{\infty}(x-y) = -\frac{1}{E_0}\delta(x-y) \tag{1.12}$$

where function δ is the unitary impulse and it is called the Dirac distribution.

Using (1.12), Equation (1.11) leads to:

$$\varepsilon_1(x) = -\frac{1}{E_0}\int_{-\infty}^{\infty} \delta(x-y)E_1(y)\varepsilon(y)dy \tag{1.13}$$

The convolution theorem states that $\int_{-\infty}^{\infty} f(x)\delta(x-a) = f(a)$ [4]. Therefore, adding $\varepsilon_0(x)$ to both sides of equation, Equation 1.11 can be modified to following form:

$$\varepsilon_0(x) + \varepsilon_1(x) = -\frac{E_1(x)}{E_0(x)}\varepsilon(x) + \varepsilon_0(x) \tag{1.14}$$

Finally, after some simple algebraic manipulations, it leads to:

$$\frac{E_0(x) + E_1(x)}{E_0(x)}\varepsilon(x) = \varepsilon_0(x) \tag{1.15}$$

which can be declared as the exact solution of the problem stated at the beginning of this Section [2].

1.2.2 Function approximation

This Section provides information about function approximation that is used in this BPM with great benefit due to basis function qualities. In the contrary to FEM, where the medium is being decomposed into elements, the BPM depends only on the position of finite number of boundary points and the values at these points.

Following Figure 1.1 shows one dimensional discretization with regular grid in the interval $\langle a, b\rangle$ evenly divided into N nodes. The first point is set at the beginning of the interval ($x_1 = a$) and the last point at the end of the interval ($x_N = b$). The rest of the nodes are regularly distributed into the interval. So the difference between two adjacent points is $h = \frac{b-a}{N-1}$.

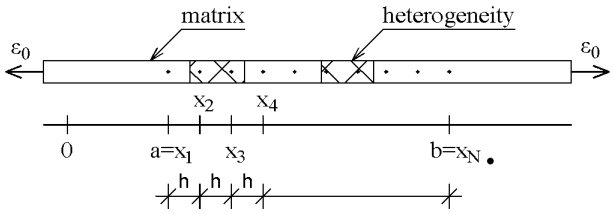

Figure 1.1: Discretization of one dimensional rod into regular grid

For approximation, the following function is being used:

$$\varphi(x) = \frac{1}{\sqrt{\pi H}} e^{-\frac{|x|^2}{Hh^2}} \tag{1.16}$$

where h is a difference between coordinates of two adjacent points as stated above and H is the dimensionless operator regulating the Gauss "hat" opening (corresponding with variance parameter in the case of Gauss probability function). Figure 1.2 shows the influence of H parameter on basis function $\varphi(x)$ while value $h = 0.2$ is kept constant. For comparison, next Figure 1.3 shows the influence of h value on basis function $\varphi(x)$ while parameter $H = 1$ is kept constant

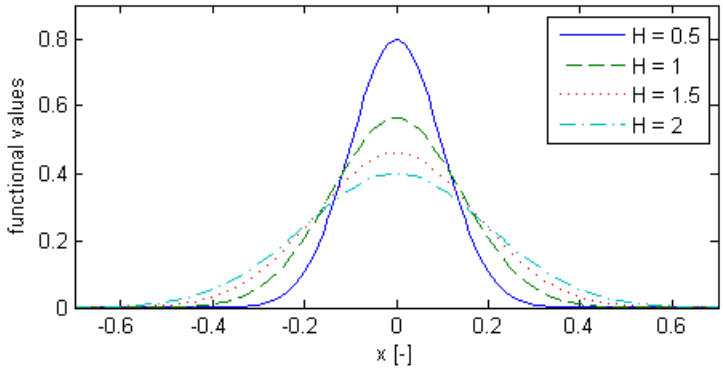

Figure 1.2: Influence of H parameter on basis function $\varphi(x)$, $h = 0.2$

The function $f(x)$ that is being approximated is expressed at an interval $\langle a, b\rangle$ as a linear combination of basis function $\varphi(x)$. The formulation is expressed as follows:

$$f(x) \approx \sum_{i=1}^{N} \alpha_i \varphi(x - x_i) \tag{1.17}$$

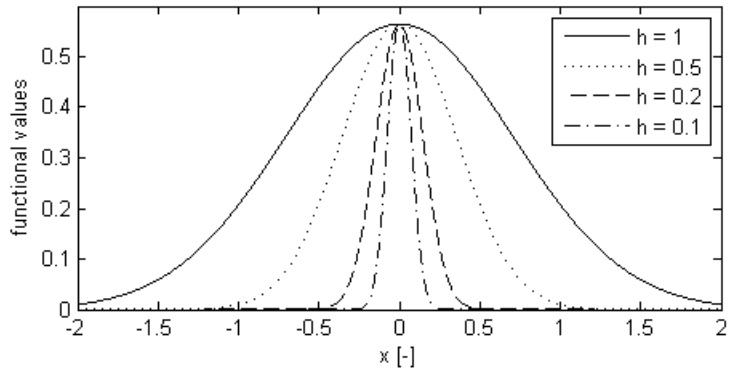

Figure 1.3: Influence of h value on basis function $\varphi(x)$, $H = 1$

where $\alpha_i \in \mathbb{R}$ are coefficients of approximation.

The function approximation consist in finding the coefficients α_i. As we have N unknown variables we need to set N linear equations that are linearly independent. To obtain these equations the equality at each point of discretization grid is required. Hence the j^{th} point determines the j^{th} equation that can be described as follows:

$$\sum_{i=1}^{N} \alpha_i \varphi(x_j - x_i) = f(x_j) \tag{1.18}$$

There is a possibility to rewrite all of the equations for determining α_i coefficients in matrix notation:

$$\boldsymbol{A}\boldsymbol{x}^{\boldsymbol{T}} = \boldsymbol{b}^{\boldsymbol{T}} \tag{1.19}$$

where $\boldsymbol{A} \in \mathbb{R}^{N \times N}$ is matrix that is determined as follows $\boldsymbol{A} = A(j,i) = \varphi(x_j - x_i)$, for $i, j = 1, 2, 3, \ldots, N$ and $\boldsymbol{x}, \boldsymbol{b} \in \mathbb{R}^N$ are both vectors with entries $\boldsymbol{x} = (\alpha_1, \alpha_2, \alpha_3, \ldots, \alpha_N)$, $\boldsymbol{b} = \big(f(x_1), f(x_2), f(x_3), \ldots, f(x_N)\big)$. The full form of matrix equation is written here:

$$\begin{pmatrix} \varphi(x_1 - x_1) & \varphi(x_1 - x_2) & \ldots & \varphi(x_1 - x_N) \\ \varphi(x_2 - x_1) & \varphi(x_2 - x_2) & \ldots & \varphi(x_2 - x_N) \\ \vdots & \vdots & \ddots & \vdots \\ \varphi(x_N - x_1) & \varphi(x_N - x_2) & \ldots & \varphi(x_N - x_N) \end{pmatrix} \begin{pmatrix} \alpha_1 \\ \alpha_2 \\ \vdots \\ \alpha_N \end{pmatrix} = \begin{pmatrix} f(x_1) \\ f(x_2) \\ \vdots \\ f(x_N) \end{pmatrix} \tag{1.20}$$

Noting that $\varphi(x)$ is even function[1] and at the interval $\langle 0, \infty)$ the function is descending, the matrix $\boldsymbol{A}$ possesses a specific structure:

$$\boldsymbol{A} = \begin{pmatrix} a_1 & a_2 & \ldots & a_{N-1} & a_N \\ a_2 & a_1 & \ldots & a_{N-2} & a_{N-1} \\ \vdots & \vdots & \ddots & \vdots & \vdots \\ a_{N-1} & a_{N-2} & \ldots & a_1 & a_2 \\ a_N & a_{N-1} & \ldots & a_2 & a_1 \end{pmatrix} \tag{1.21}$$

[1]Even function is defined as follows: $\forall x \in \mathbb{R}, \varphi(-x) = \varphi(x)$.

where $A(j,i) = a_{|i-j|+1} = \varphi(x_i - x_j)$. This matrix is symetric Toeplitz matrix with a property:

$$\forall i,j = 1,2,3,\ldots,N; i < j \Rightarrow a_i > a_j.$$

1.2.3 Problem solution

This Section provides finallization of the BPM description using function approximation from Section 1.2.2. To complete this method we have to continue with last Equation (1.15) from Section 1.2.1. For lucidity the equation is rewritten here:

$$\frac{E_0(x) + E_1(x)}{E_0(x)}\varepsilon(x) = \varepsilon_0(x) \tag{1.22}$$

To solve this equation the unknown function $\varepsilon(x)$ is approximated using approximation function $\varphi(x)$ as in the Section 1.2.2. The rewritten Equation (1.22) now looks as follows:

$$\frac{E_0(x) + E_1(x)}{E_0(x)} \sum_{i=1}^{N} \alpha_i \varphi(x - x_i) = \varepsilon_0(x) \tag{1.23}$$

It is apparent that the equilibrium at each point with coordinate x_j, for $j = 1,2,3,\ldots,N$ leads to N equations. The j^{th} row of the system can be written as:

$$\frac{E_0(x_j) + E_1(x_j)}{E_0(x_j)} \sum_{i=1}^{N} \alpha_i \varphi(x_j - x_i) = \varepsilon_0(x_j) \tag{1.24}$$

Hence it can be recast in the matrix form:

$$\big(\boldsymbol{C}\boldsymbol{A}\big)\boldsymbol{x}^{\boldsymbol{T}} = \boldsymbol{b}^{\boldsymbol{T}} \tag{1.25}$$

where individual matrices are written below:

$$\boldsymbol{C} = \begin{pmatrix} \frac{E_0+E_1(x_1)}{E_0} & 0 & \ldots & 0 \\ 0 & \frac{E_0+E_1(x_2)}{E_0} & \ldots & 0 \\ \vdots & \vdots & \ddots & \vdots \\ 0 & 0 & \ldots & \frac{E_0+E_1(x_N)}{E_0} \end{pmatrix} \tag{1.26}$$

$$\boldsymbol{A} = \begin{pmatrix} \varphi(x_1 - x_1) & \varphi(x_1 - x_2) & \ldots & \varphi(x_1 - x_N) \\ \varphi(x_2 - x_1) & \varphi(x_2 - x_2) & \ldots & \varphi(x_2 - x_N) \\ \vdots & \vdots & \ddots & \vdots \\ \varphi(x_N - x_1) & \varphi(x_N - x_2) & \ldots & \varphi(x_N - x_N) \end{pmatrix} \tag{1.27}$$

$$\boldsymbol{x} = \begin{pmatrix} \alpha_1 & \alpha_2 & \ldots & \alpha_N \end{pmatrix} \tag{1.28}$$

$$\boldsymbol{b} = \begin{pmatrix} \varepsilon_0(x_1) & \varepsilon_0(x_2) & \ldots & \varepsilon_0(x_N) \end{pmatrix} \tag{1.29}$$

The last equation can be written in slightly different way:

$$\boldsymbol{A}\boldsymbol{x}^{\boldsymbol{T}} = \boldsymbol{C}\boldsymbol{b}^{\boldsymbol{T}} \tag{1.30}$$

$$\boldsymbol{A}\boldsymbol{x}^{\boldsymbol{T}} = (\boldsymbol{c} \odot \boldsymbol{b})^{\boldsymbol{T}} \tag{1.31}$$

where all of the notation is the same except binary operator $\odot$ meaning product by product matrix multiplication (for $\boldsymbol{A}, \boldsymbol{B} \in T^{n\times m}$, $\boldsymbol{AB} = \boldsymbol{C} = C(i,j) = A(i,j)B(i,j)$, for $i = 1, 2, \ldots, n$ and $j = 1, 2, \ldots, m$) and the array $\boldsymbol{c} \in \mathbb{R}^{1\times N}$ written below:

$$\boldsymbol{c} = \begin{pmatrix} \frac{E_0}{E_0+E_1(x_1)} & \frac{E_0}{E_0+E_1(x_2)} & \cdots & \frac{E_0}{E_0+E_1(x_N)} \end{pmatrix} \tag{1.32}$$

1.3 Fast Fourier Transform Based Method

This Section provides theoretical approach to the Fast Fourier Transform Based Method. Information about this method are gained from Michel [3]. It is based on analyzing periodically repeating medium with heterogeneities. In this thesis one dimensional case is considered and similarly to previous BPM the cross-section is unitary and thus it is not included in the formulas. The medium is composed from basic cell which is characterized with $E(x)$ stiffness defined at the interval $\langle a, b\rangle$ (a, b are boundary points of the cell) and the boundary condition for deformation have to be satisfied. It means that:

$$\varepsilon(a) = \varepsilon(b) \tag{1.33}$$

The infinite one dimensional rod is loaded with average deformation ε_0. For the needs of the FFT based method the deformation along the rod $\varepsilon(x)$ is decomposed into:

$$\varepsilon(x) = \varepsilon_0 + \varepsilon_1(x) \tag{1.34}$$

where $\varepsilon_1(x)$ is a complement to $\varepsilon(x)$ deformation along the rod. It is necessary to note that the deformations ε_0, $\varepsilon_1(x)$ have different sense than in the BPM.

To obtain some information about $\varepsilon_1(x)$ deformation the equation $\varepsilon_1(x) = \frac{d}{dx}u_1(x)$ is adjusted using integration by parts:

$$\varepsilon_1(x) = \frac{d}{dx}u_1(x) \Rightarrow \int_a^b \varepsilon_1(x)dx = \int_a^b \frac{d}{dx}u_1(x)dx = \big[u_1(x)\big]_a^b = u_1(b) - u_1(a) \tag{1.35}$$

Moreover, noting that the term $\big(u_1(b) - u_1(a)\big)$ has to be equal to zero due to boundary condition at basic cell boundaries. Hence, the everage $\varepsilon_1(x)$ deformation at the cell is equal to zero.

To analyse one dimensional rod with FFT based method, the approach with the Green function is used similarly to the case of the BPM. Hence, the equilibrium state is described with the following equation:

$$\frac{d}{dx}\Big(E(x)\varepsilon(x)\Big) = 0 \tag{1.36}$$

For the use of the method the $(E_H - E_H)$ term is added to the equation. The stiffness E_H is an auxiliary value of the analogical homogeneous problem with same deformations ε_0, $\varepsilon_1(x)$ and the same boundary condition. Hence Equation (1.36) follows:

$$\frac{d}{dx}\Big[\Big(E_H - E_H + E(x)\Big)\varepsilon(x)\Big] = 0 \tag{1.37}$$

$$\frac{d}{dx}\Big(E_H\varepsilon(x)\Big) = -\frac{d}{dx}\Big[\Big(E(x) - E_H\Big)\varepsilon(x)\Big] \tag{1.38}$$

The $\varepsilon(x)$ at the left side of the last equation can be decomposed. Next we can notice that $\frac{d}{dx}\big(E_H\varepsilon_0\big) = 0$ as it is derivation of constant. Hence Equation (1.38) leads to:

$$\frac{d}{dx}\Big(E_H\varepsilon_1(x)\Big) = -\frac{d}{dx}\Big[\Big(E(x) - E_H\Big)\varepsilon(x)\Big] \tag{1.39}$$

The left side of the equation can be interpreted as homogeneous rod deformed with $\varepsilon_1(x)$ deformation. Hence, the right side of the equation can be interpreted as generalized load $f(x)$ causing that $\varepsilon_1(x)$ deformation:

$$f(x) = -\frac{d}{dx}\Big[\Big(E(x) - E_H\Big)\varepsilon(x)\Big] \tag{1.40}$$

Now we can take a look at $u_1(x)$ displacement using Green function. In the case of the FFT based method an integral is defined at interval $\langle a, b\rangle$, hence:

$$u_1(x) = \int_a^b G(x,y)f(y)dy \tag{1.41}$$

After derivation and substitution with Equation (1.40), it leads to:

$$\varepsilon_1(x) = -\int_a^b \frac{\partial G(x,y)}{\partial x}\frac{d}{dy}\Big[\Big(E(y) - E_H\Big)\varepsilon(y)\Big]dy \tag{1.42}$$

Integration by parts heads to:

$$\varepsilon_1(x) \overset{P.P.}{=} \int_a^b \frac{\partial^2 G(x,y)}{\partial x \partial y}\Big(E(y) - E_H\Big)\varepsilon(y)dy - \frac{\partial G(x,y)}{\partial x}\frac{d}{dx}\Big[\Big(E(y) - E_H\Big)\varepsilon(y)\Big]\Big|_a^b \tag{1.43}$$

the second term at the right side of equation is equal to zero due to identical deformation at cell boundaries.

Next we can rewrite term $\frac{\partial^2 G(x,y)}{\partial x \partial y}$ noting that the variables x and y depends just on their difference, we can say that $\frac{\partial^2 G(x,y)}{\partial x \partial y} = K^{per}(x-y)$. Hence, it follows as:

$$\varepsilon_1(x) = \int_a^b K^{per}(x-y)\Big(E(y) - E_H\Big)\varepsilon(y)dy \tag{1.44}$$

The interpretation of function $K^{per}(x-y)$ using Fourier Transform has to satisfy two conditions. The first condition says that $K^{per}(x-y) = \frac{1}{E_0}\delta(x-y)$ and the second one declare that the average $\varepsilon_1(x)$ deformation is equal to zero:

$$\int_a^b \varepsilon_1(x)dx = 0$$

Both conditions can be proved using the Fourier Transform.

Hence, we can rewrite Equation (1.44) to the following form satisfying both conditions:

$$\varepsilon_1(x) = \frac{E(x) - E_H}{E_H}\varepsilon(x) - \frac{1}{b-a}\int_a^b \frac{E(y) - E_H}{E_H}\varepsilon(y)dy \tag{1.45}$$

To apply this equation to practical use it is necessary to provide some other emendations. Firstly we have to discretize the interval into N nodes that change the integral over continuous field into the sum. It is necessary to note that the discretization leads to a loss in exactness over the continuous field. The same approach of discretization as in the case of BPM is being used. Hence the first point is set at the beginning of the interval ($x_1 = a$) and the last point at the end of the interval ($x_N = b$). The rest of the nodes are regularly distributed into the interval, so the difference between coordinates of two adjacent points is $h = \frac{b-a}{N-1}$. This discretization change Equation (1.45) to:

$$\varepsilon_1(x_j) = \frac{E(x_j) - E_H}{E_H}\varepsilon(x_j) - \frac{1}{N}\sum_{i=1}^{N} \frac{E(x_i) - E_H}{E_H}\varepsilon(x_i), \quad \text{for } j = 1, 2, \ldots, N \tag{1.46}$$

The second modification has to be done with the stiffness E_H as it is auxiliary value of imaginary case of homogeneous rod it cannot be known until the deformation of the rod is calculated. Hence the E_H stiffness is estimated with some reference stiffness E_{ref}. The inaccurate estimation of this E_{ref} value leads to inexact solution of the deformation thus the iteration approach to solution has to be applied. The appropriate setting of the E_{ref} value is the main point of the efficiency or even successfulness of the iteration method.

Using Equation (1.46) the k^{th} iteration of the algorithm can be written as:

$$\varepsilon_1^{k+1}(x_j) = \frac{E(x_j) - E_{ref}}{E_{ref}}\varepsilon^k(x_j) - \frac{1}{N}\sum_{i=1}^{N} \frac{E(x_i) - E_{ref}}{E_{ref}}\varepsilon^k(x_i), \quad \text{for } j = 1, 2, \ldots, N \tag{1.47}$$

It is necessary to note that the initial $\varepsilon_1^0(x)$ deformation is set to:

$$\varepsilon_1^0(x) = 0$$

The convergence of the iteration method is not the aim of this project hence it is not provided. The practical algorithm used for the analysis of the method is provided in Section 2.2.

Chapter 2

Methodology

This Chapter provides information about procedure of analysis of individual methods. The division into sections is done accordingly to Chapter 1 Theory and Chapter 3 Results. Hence, firstly the Boundary Point Method is discussed in Section 2.1 and after that Fast Fourier Transform Based Method in Section 2.2. Each section provides information about parameters of method that are analysed, about the algorithm that is used for calculation and the functions that are analysed. It is necessary to note that all of the calculation were done in `MATLAB R2007a`.

2.1 Boundary Point Method

Similarly to Chapter 1, the discussion about the BPM method is divided into Section 2.1.1 dealing with function approximation and Section 2.1.2 dealing with deformation of one dimensional rod with heterogeneities.

2.1.1 Function approximation

This part provides information about the method that is used in this project to approximate some particular function with base functions. Firstly, the inputs to the method are summarized. All of the inputs are divided into internal parameters:

- N — number of nodes used for discretization of the interval $\langle a, b\rangle$
- H — the parameter of approximation function $\varphi(x)$

and other inputs that are following:

- $f(x)$ — function that is being approximated with constant a and b as the end points of the interval where the function is defined
- $\varphi(x)$ — base function that is used for approximation
- s — parameter for norm calculation determining the step between two adjacent points were the norm is calculated

Algorithm used for approximation is described in individual steps:

1. definition of the approximation function $f(x)$ at interval $\langle a, b\rangle$, defining the base function $\varphi(x)$ and setting of parameters N, H, s
2. calculation of $h = \frac{b-a}{N-1}$
3. discretizing the definitional interval $\langle a, b\rangle$ into N nodes, each node is assigned to coordinate with transform $N \xrightarrow{g} \langle a, b\rangle$ that is described as $g(i) = x_i = hi$, for $i = 1, 2, 3, \ldots, N$
4. determination of the array $\boldsymbol{b} = \big(f(x_1), f(x_2), \ldots, f(x_N)\big)$
5. determination of matrix $\boldsymbol{A} = A(j, i) = \varphi(x_i - x_j) = \varphi(hi - hj)$ for $i, j = 1, 2, 3, \ldots, N$
6. calculation of the matrix equation $\boldsymbol{A}\boldsymbol{x}^{\boldsymbol{T}} = \boldsymbol{b}^{\boldsymbol{T}}$ for unknown array $\boldsymbol{x} = (\alpha_1, \alpha_2, \ldots, \alpha_N)$
7. interpretation of the data consisting of calculation approximation function $\bar{f}$ at arbitrary point x, $\bar{f}(x) = \sum_{i=1}^{N} \alpha_i \varphi(x - hi)$
8. calculation of differences between the function $f(x)$ and the function $\bar{f}(x)$ using ℓ^2 norm (2.1) and maximal norm (2.2).

The ℓ^2 norm and maximal norm is calculated at interval $\langle a, b\rangle$ as follows:

$$\big\|f(x) - \bar{f}(x)\big\|_2 = \frac{\sum\limits_{x \in \boldsymbol{G}} \big(f(x) - \bar{f}(x)\big)^2}{\frac{b-a}{s}} \tag{2.1}$$

$$\big\|f(x) - \bar{f}(x)\big\|_{max} = \frac{\max\limits_{x \in \boldsymbol{G}} \big|f(x) - \bar{f}(x)\big|}{\max\limits_{x \in \boldsymbol{G}} \big|f(x)\big|} \tag{2.2}$$

where $\boldsymbol{G} = \big\{x \in \langle a, b\rangle; x = a + sn, n \in \mathbb{Z}\big\}$ is a set for norm calculation ($\mathbb{Z}$ is the set of all integer numbers). To increase the accuracy of the norm it is necessary to decrease the parameter s. In the case of this project the s parameter was set to value 0.0005. This value means that the norm is calculated in at least 5 points between two adjacent nodes of discretization grid hence it guarantees the sufficient accuracy.

Here we provides information about the concrete values used in this project. For the parametric study the functions that are shown in Figure 2.1 is chosen. The functions $f_i(x)$, $i = 1, 2, 3$ are defined at interval $\langle -1, 2\rangle$. All of the functions $f_i(x)$ are equal to zero at set $\langle -1, 2) \bigcup (-1, 2\rangle$ and at the interval $\langle 0, 1\rangle$ there is defined some particular nonzero function. As the first type of function is used constant function $f_1(x) = 0$ (dashed line), the second type is a function $f_2(x) = \sin(\pi x)$ (full line) and finally the third function is piecewise constant defined as follows (dash-and-dot line):

$$\begin{aligned} f_3(x) = 1, \quad \text{at the set} \quad & \langle 0.11, 0.22) \bigcup \langle 0.33, 0.44) \bigcup \\ & \bigcup \langle 0.55, 0.66) \bigcup \langle 0.70, 0.78) \bigcup \langle 0.82, 0.95) \\ f_3(x) = 0, \quad \text{otherwise.} & \end{aligned}$$

The same type of lines for particular functions are used also in Section 3.1.1 where the results of the analysis are provided.

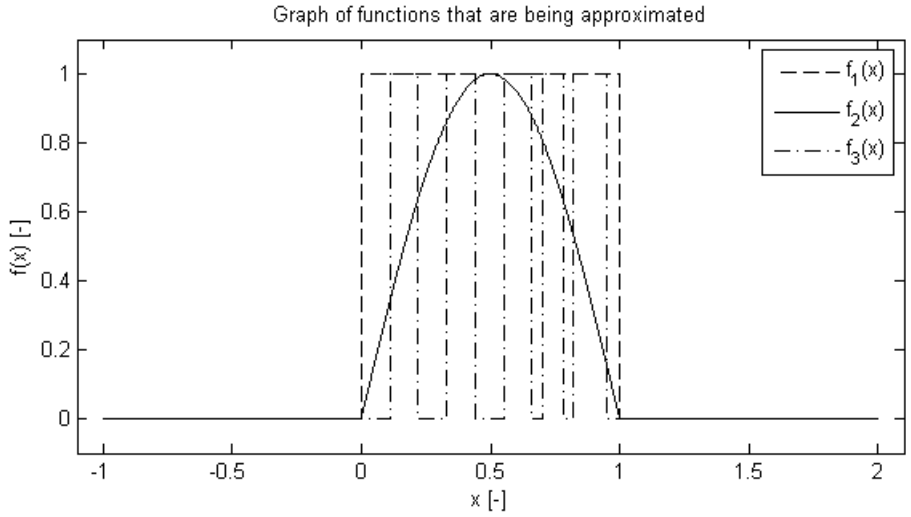

Figure 2.1: Graph of functions that are being approximated

2.1.2 Deformation analysis of one dimensional rod

This part provides information about the algorithm based on the BPM. First we have to specify what inputs to the method. We can divide all of the inputs into internal parameters of the method:

- N — number of nodes used for discretization of the interval $\langle a, b\rangle$
- H — the parameter of approximation function $\varphi(x)$

and other inputs that are following:

- $E_0(x)$, $E_1(x)$ — the stiffnesses of analyzed medium at interval $\langle a, b\rangle$, $E_0(x) = \text{const.}$, $E_1(x) \neq \text{const.}$ (in the algorithm the ratio $p = \max_{x\in\langle a,b\rangle} \frac{E_1(x)}{E_0(x)}$ is analysed)
- $\varphi(x)$ — basis function used for approximation
- s — parameter for norm calculation determining the step between two adjacent points were the norm is calculated

Algorithm used for analysing one dimensional rod with BPM is written below in individual steps:

1. definition of the stiffness and initial deformation functions $E_0(x)$, $E_1(x)$ resp. $\varepsilon_0(x)$, $\varepsilon_0(x)$ at interval $\langle a, b\rangle$
2. setting N, H, s parameters and defining the basis function for approximation $\varphi(x)$
3. calculation of $h = \frac{b-a}{N-1}$
4. discretizing the definitional interval $\langle a, b\rangle$ into N nodes, each node is assigned to coordinate with transform $N \xrightarrow{g} \langle a, b\rangle$ that is described as $g(i) = x_i = hi$, for $i = 1, 2, 3, \ldots, N$
5. determination of matrix $\boldsymbol{A} = A(j, i) = \frac{E_0(x_i)+E_1(x_i)}{E_0(x_i)}\varphi(x_i - x_j)$ for $i, j = 1, 2, 3, \ldots, N$

6. calculation of the matrix equation $\boldsymbol{A}\boldsymbol{x}^{\boldsymbol{T}} = \boldsymbol{b}^{\boldsymbol{T}}$ for unknown array $\boldsymbol{x} = (\alpha_1, \alpha_2, \ldots, \alpha_N)$
7. interpretation of the data consisting of calculation deformation $\bar{\varepsilon}(x)$ approximated with base functions at arbitrary point x, $\bar{\varepsilon}(x) = \sum_{i=1}^{N} \alpha_i \varphi(x - hi)$
8. calculation of the real deformation $\varepsilon_{real}(x)$ using analytical solution, hence $\varepsilon_{real}(x) = \frac{E_0(x)\varepsilon_0(x)}{E_0(x)+E_1(x)}$
9. calculation of differences between the function $\bar{\varepsilon}(x)$ obtained from BPM algorithm and the function $\varepsilon(x)$ gained from analytical solution using ℓ^2 norm (2.3).

$$\left\|\varepsilon(x) - \bar{\varepsilon}(x)\right\|_2 = \frac{\sum_{x \in \boldsymbol{G}} \left(\varepsilon(x) - \bar{\varepsilon}(x)\right)^2}{\frac{b-a}{s}} \tag{2.3}$$

where $\boldsymbol{G} = \left\{x \in \langle a, b\rangle; x = a + sn, n \in \mathbb{Z}\right\}$ is a set for norm calculation ($\mathbb{Z}$ is the set of all integer numbers).

Here we provide information about the concrete values used in this project. To analyse this method we have chosen the following parameters:

- the stiffness of periodic medium is defined as $E(x) = E_0 + E_1(x)$, where the function $E_0 = 10$ is stiffness of matrix and $E_1(x)$ is the complement to heterogeneities stiffness. The function $E_1(x)$ is defined as follows: $E_1(x) = pE_0 f_i(x)$, where $f_i(x)$, $i = 1, 2, 3$ are functions defined in Section 2.1.1, $p = 5, 100$, the functions $E(x)$ used for the analysis are provided in Section 3 Results
- the rod described with the stiffness is discretized at interval $\langle -1, 2\rangle$
- number of nodes N used for discretization was set to values $N = 64, 256$
- the s parameter for convergence calculation is set to value 0.0005 as in the case of function approximation
- setting of initial deformations $\varepsilon_0 = 1$ at the infinity points of the rod

2.2 Fast Fourier Transform Based Method

This section provide information about the algorithm of the FFT-Based Method. The structure of this section follows the previous sections, hence first we define the internal input parameters of the method that are:

- N — number of nodes using for discretization of the medium
- E_{ref} — the value of reference stiffness
- ζ — the parameter of convergence - the iteration algorithm continue until the convergence criterium is satisfied
- ζ_{max} — the parameter of divergence - the iteration algorithm continue until the divergence criterium is satisfied

and other inputs are:

- $E(x)$ — the Young modulus of periodic cell
- $\varepsilon_0(x)$, $\varepsilon_1(x)$ — deformations of periodic cell

Algorithm used for approximation is written below in individual steps:

1. defining the $E(x)$ stiffnesses at interval $\langle a, b\rangle$
2. setting the $k = 0$ meaning the number of iterations
3. setting the initial deformation $\varepsilon_0(x)$ and $\varepsilon_1^0(x)$ at interval $\langle a, b\rangle$
4. setting of internal parameters N and E_{ref}
5. calculation of $h = \frac{b-a}{N-1}$
6. discretizing the definitional interval $\langle a, b\rangle$ into N nodes, each node is assigned to coordinate with transform $N \xrightarrow{g} \langle a, b\rangle$ that is described as $g(i) = x_i = hi$, for $i = 1, 2, 3, \ldots, N$
7. setting $k = k + 1$
8. calculation of polarization stress in each point of discretization grid using following formula: $\sigma_{pol}(x_i) = \big(E(x_i) - E_{ref}\big)\big(\varepsilon_0(x_i) + \varepsilon_1^k(x_i)\big)$, for $i = 1, 2, 3, \ldots, N$
9. calculation primal deformation using following formula: $\varepsilon_{1_{prim}}(x_i) = \frac{\sigma_{pol}(x_i)}{E_{ref}}$
10. calculation mean of primal deformation $\bar{\varepsilon}_{1_{prim}} = \frac{1}{N}\sum_{i=1}^{N}\varepsilon_{1_{prim}}(x_i)$
11. calculation $\varepsilon_1^k(x_i) = \varepsilon_{1_{prim}}(x_i) - \bar{\varepsilon}_{1_{prim}}$
12. calculation of the convergence using max norm: $\left\|\varepsilon_1^k(x) - \varepsilon_1^{k-1}\right\|_{max} = \frac{\max\limits_{x=x_1,x_2,\ldots,x_N}\left|\varepsilon_1^k(x) - \varepsilon_1^{k-1}\right|}{\varepsilon_0(x)}$
13. if the condition $\left\|\varepsilon_1^k(x) - \varepsilon_1^{k-1}\right\|_{max} > \zeta_{max}$ is satisfied the algorithm stops and it is declared as divergence (hence the algorithm has to be launched again with more appropriate value of parameter E_{ref})
14. if the condition $\left\|\varepsilon_1^k(x) - \varepsilon_1^{k-1}\right\|_{max} < \zeta$ is not satisfied the algorithm go back to the step 7., otherwise the algorithm continue with next step as usual
15. calculation of total deformation $\varepsilon(x_i) = \varepsilon_0(x_i) + \varepsilon_1^k(x_i)$, for $i = 1, 2, 3, \ldots, N$
16. calculation of total stress $\sigma(x_i) = E(x_i)\varepsilon(x_i)$, for $i = 1, 2, 3, \ldots, N$

Here we provide information about the concrete values used in this project. To analyse this method we have chosen the following parameters:

- the stiffness of periodic medium is defined as $E(x) = E_0 + E_1(x)$, where the function $E_0 = 10$ is stiffness of matrix and $E_1(x)$ is the complement to heterogeneities stiffness. The function $E_1(x)$ is defined as $E_1(x) = pE_0 f_i(x)$, where $f_i(x)$, $i = 1, 2, 3$ are functions defined in Section 2.1.1, $p = 5, 100$, the functions $E_(x)$ are plotted for each case in the Section 3 Results

- the one dimensional rod was discretized at interval $\langle -1, 2 \rangle$
- the parameter s determining the step of convergence was set to 0.0005
- number of nodes N used for basic cell discretization was set to values $N = 64, 256$
- setting of initial deformations, in our case $\varepsilon_0(x) = 1$ and $\varepsilon_1(x) = 0$ are taken into the algorithm

Chapter 3

Results

This chapter summarizes information obtained when analysing both meshless methods. Section 3.1 provides information about the Boundary Point Method and Section 3.2 about the Fast Fourier Transform Based Method.

3.1 Boundary Point Method

This section, providing information about the BPM, is divided into Section 3.1.1 describing the approximation of functions and into Section 3.1.2 dealing with deformation analysis of a one dimensional rod.

3.1.1 Function approximation

This section deals with function approximation that plays the main role in deformation analysing of one dimensional rod. The function approximation is based on replacement of linear combination of the basis functions

$$\varphi(x) = \frac{1}{\sqrt{\pi H}} e^{-\frac{|x|^2}{Hh^2}}$$

as it is described in Section 1.2.2 in detail. The main role in function approximation plays the parameter H and the number of dicretization points N.

The approximation was tested on three particular functions $f_1(x)$, $f_2(x)$ and $f_3(x)$ that are described in Section 2.1.1. As a accuracy criterion of approximation the ℓ^2 and maximal norm were used. Thus following Figures 3.1, 3.2 and 3.3 show the accuracy of approximation for 64, 256 and 1024 discretization nodes respectively.

It is necessary to note that the accuracy increase with the decreasing norm. Focusing on upper part of figures with ℓ^2 norm we can notice that the norm dramatically decreases with increasing H parameter approximately up to the value 0.4-0.5 regardless the tested functions $f_1(x)$, $f_2(x)$ and $f_3(x)$. The next increase in the H parameter does not change the ℓ^2 norm significantly however the very slight increase in the norm could be observed. The only one significant increase can be noticed for $f_3(x)$ function discretized on the investigated interval into 64 nodes. It is caused by rapidly oscillating function values in combination with insufficient number of discretizing nodes.

The best H parameter for individual functions with regard to number of nodes N is shown in Figure 3.4 - the values for generation of this graph are provided in Table 3.1.

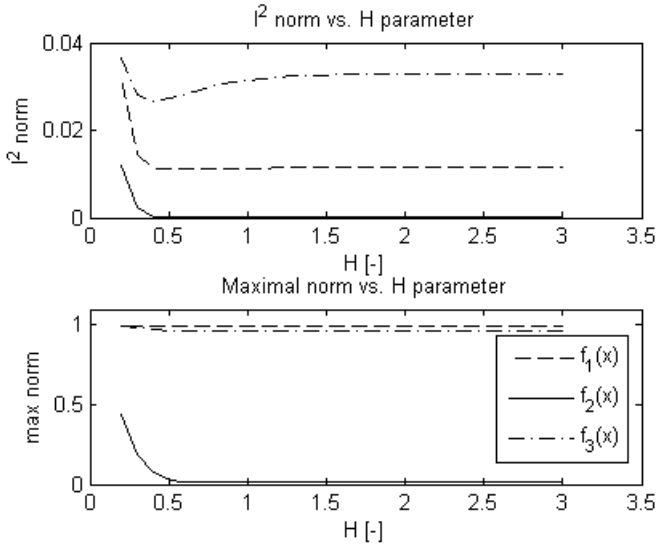

Figure 3.1: Norm of functions $f_1(x)$, $f_2(x)$ and $f_3(x)$ vs. H parameter, $N = 64$

The functions $f_1(x)$ and $f_3(x)$ have the optimal H parameter in the range 0.4-0.7 whereas the optimal value for function $f_3(x)$ varies between 0.8 and 3.3. It can be said that H parameter is not so significant for the accuracy of approximation for this function $f_3(x)$ as the norm is kept on similar value.

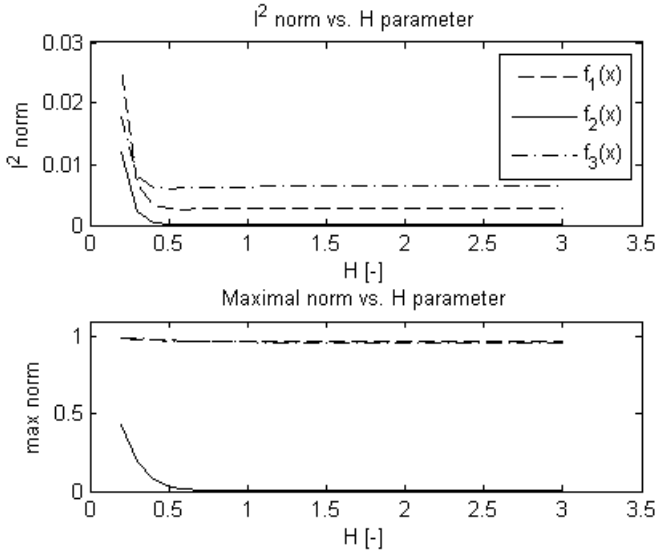

Figure 3.2: Norm of functions $f_1(x)$, $f_2(x)$ and $f_3(x)$ vs. H parameter, $N = 256$

While ℓ^2 norm provides information about overall approximation of individual functions at the interval the maximal norm provides information about the maximal absolute difference between the function and its approximation. We can notice that the maximal norm of functions $f_1(x)$ and $f_3(x)$ is kept a quite close to value 1 regardless the H parameter and the number of discretizing nodes N as well. Whereas the curve of maximal norm of function $f_2(x)$ follows the waveform of ℓ^2 norm. This phenomenon is caused by discontinuity of functions $f_1(x)$ and $f_3(x)$. For those functions the diference of one-sided

limits at the points of discontinuity is just the value 1 that is why the maximal norm is close the value 1 as the function approximation is continuous and it cannot fit the function very well at points of discontinuity. On the contrary the function $f_3(x)$ is continuous hence the maximal norm goes to zero.

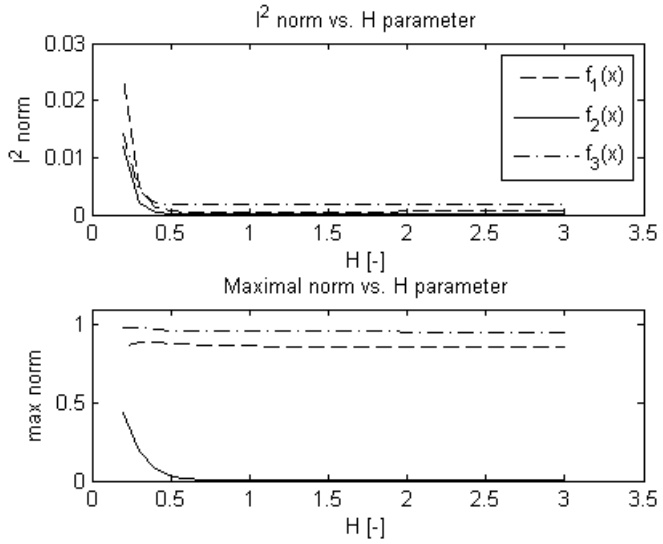

Figure 3.3: Norm of functions $f_1(x)$, $f_2(x)$ and $f_3(x)$ vs. H parameter, $N = 1024$

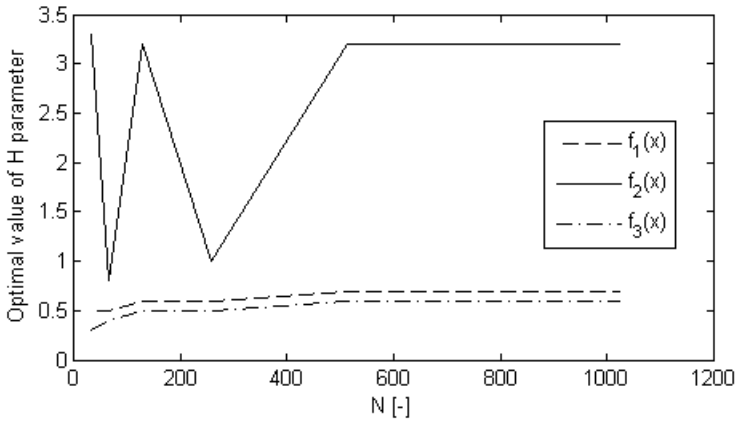

Figure 3.4: Graph of optimal H parameter vs. number of nodes N

Now we can take a look at functions being approximated with their approximations for best fit H values and different number of discretizing nodes N. For the number of nodes $N = 64$ the graph of individual base functions is also provided in the bottom part of each figure.

Figure 3.5 shows the approximation of function $f_1(x)$ for $N = 64$. It can be noticed that the function is not properly approximated at the points of discontinuity $x = 0$ and $x = 1$. This imperfection shown at the graph causes the maximal value being close to the value 1.

Figure 3.6 shows the approximation of function $f_2(x)$ for $N = 64$. It can be seen that even the small number of discretization points can provide sufficient results of function approximation. Hence the graph of function approximation is not provided for the greater

number of discretizing nodes N	32	64	128	256	512	768	1024
optimal H **parameter for** $f_1(x)$	0.5	0.5	0.6	0.6	0.7	0.7	0.7
optimal H **parameter for** $f_2(x)$	3.3	0.8	3.2	1.0	3.2	3.2	3.2
optimal H **parameter for** $f_3(x)$	0.3	0.4	0.5	0.5	0.6	0.6	0.6

Table 3.1: Values of optimal H parameter using ℓ^2 norm

number of discretization points as the function and its approximation fit together very well.

Figure 3.7 shows the approximation of function $f_3(x)$ for $N = 64$ with the base functions. In comparison with the previous graph of function $f_2(x)$ we can notice plenty of imperfections due to character of $f_3(x)$ in combination with insufficient number of discretizing points N.

Following Figures 3.8 and 3.9 show the approximation of function $f_1(x)$ for $N = 256$ and $N = 1024$ respectively. With the aid of Figure 3.5 we can study the progress of function approximation with increase number of discretizing points. The approximation works pretty good except the points of discontinuity. The particular view of that point is shown at Figure 3.10. The oscillation close to point of discontinuity is called Gibb's effect.

Analogically as the three previous figures following Figures 3.11 and 3.12 shows the approximation of function $f_3(x)$ for $N = 256$ and $N = 1024$ respectively and Figure 3.13 shows the Gibb's effect that is significant even with the increasing number of discretizing points.

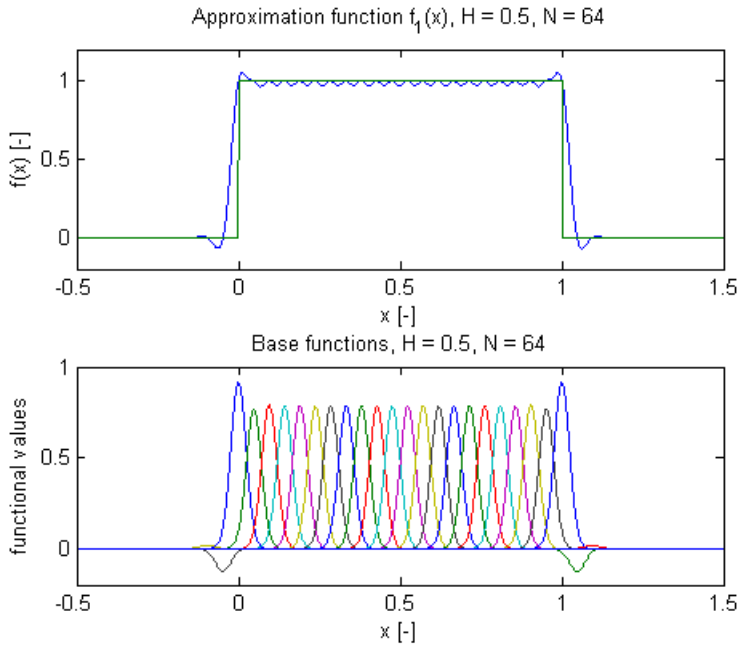

Figure 3.5: Approximated function $\bar{f}_1(x)$, $N = 64$

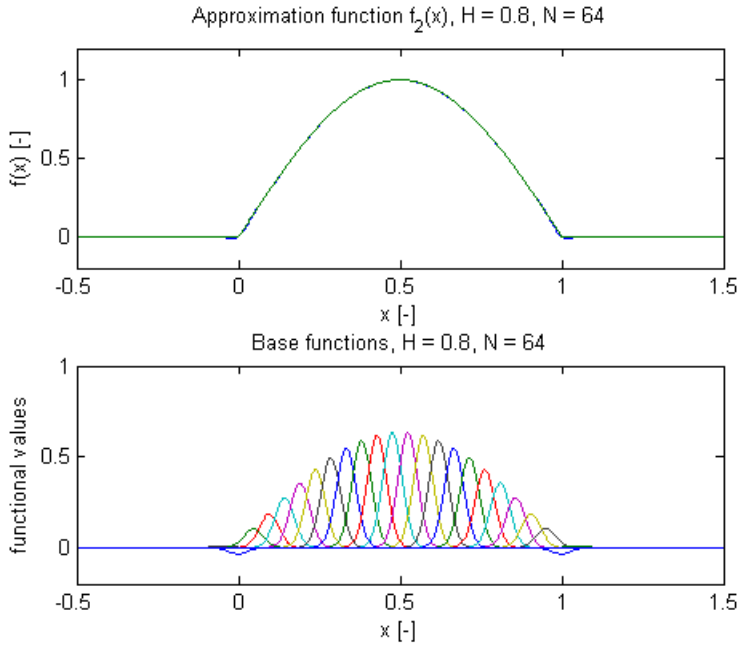

Figure 3.6: Approximated function $\bar{f}_2(x)$, $N = 64$

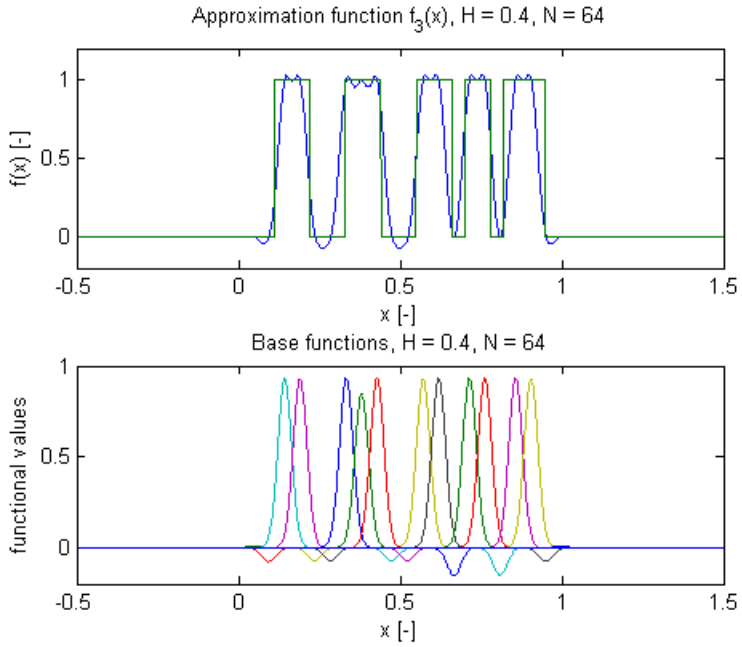

Figure 3.7: Approximated function $\bar{f}_3(x)$, $N = 64$

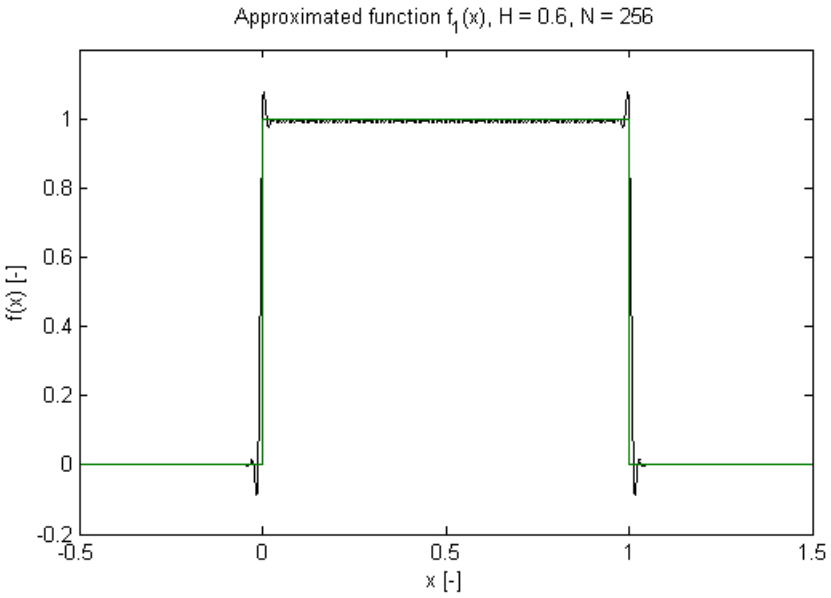

Figure 3.8: Approximated function $\bar{f}_1(x)$, $N = 256$

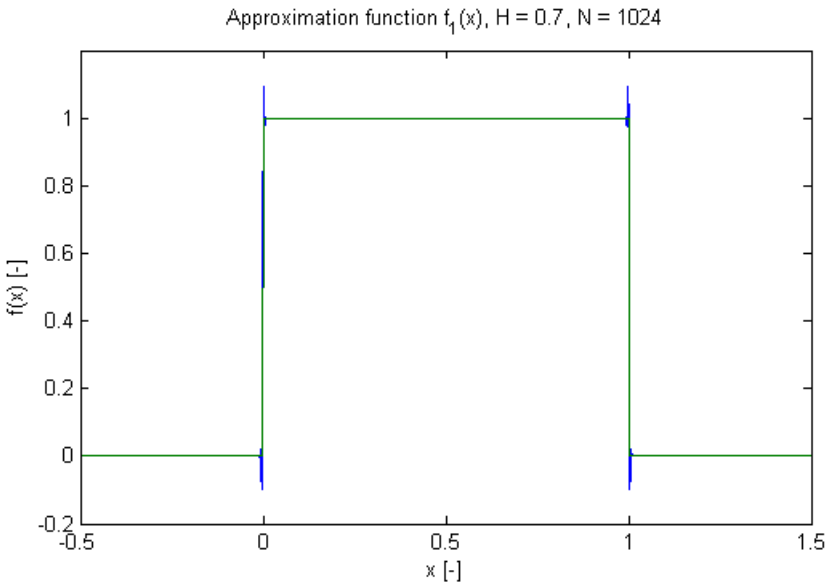

Figure 3.9: Approximated function $\bar{f}_1(x)$, $N = 1024$

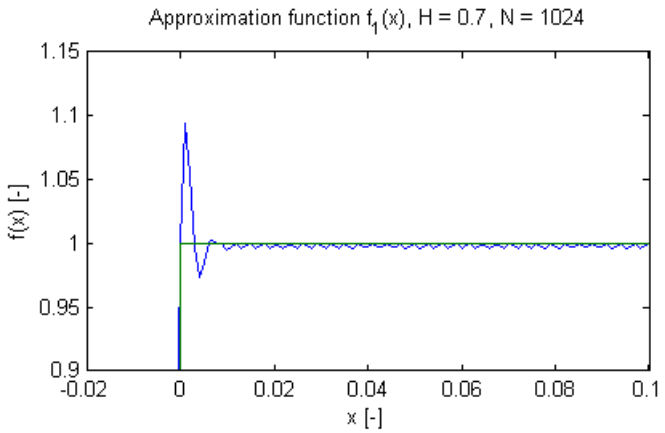

Figure 3.10: Gibb's effect of function $\bar{f}_1(x)$, $N = 1024$

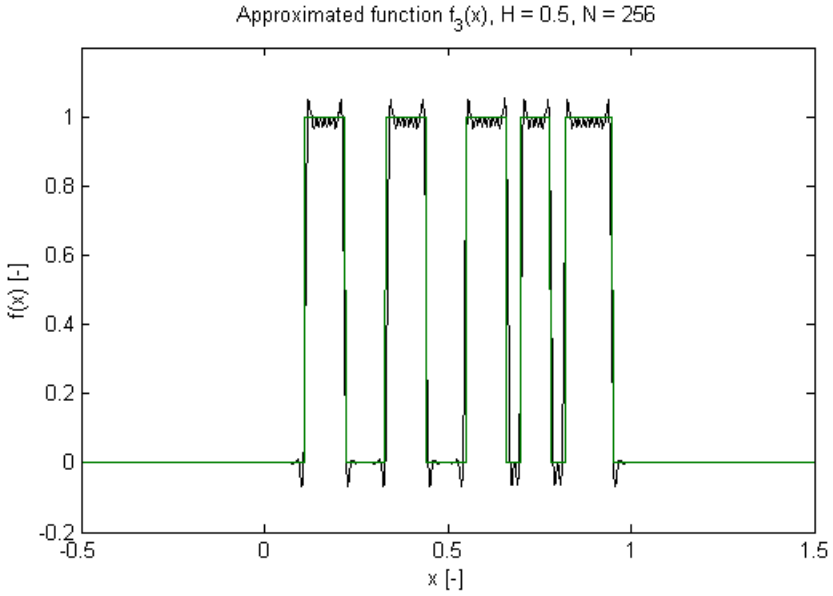

Figure 3.11: Approximated function $\bar{f}_3(x)$, $N = 256$

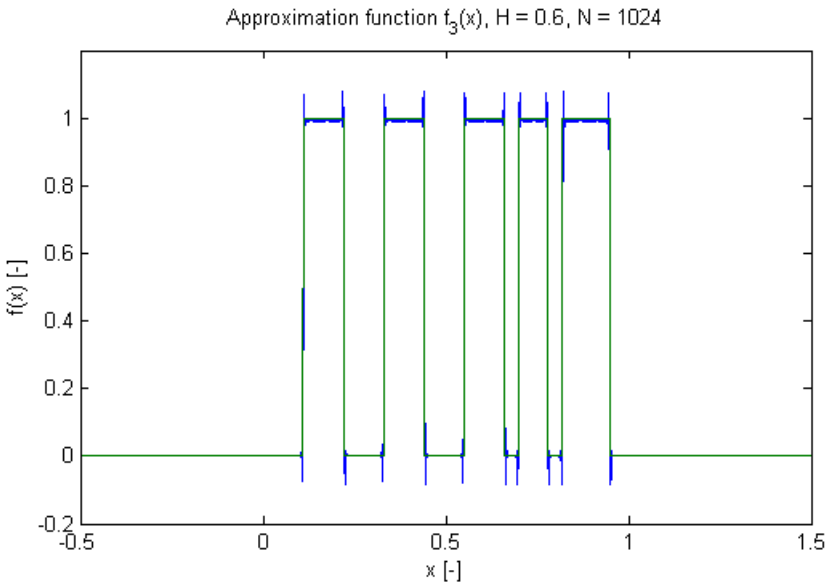

Figure 3.12: Approximated function $\bar{f}_3(x)$, $N = 1024$

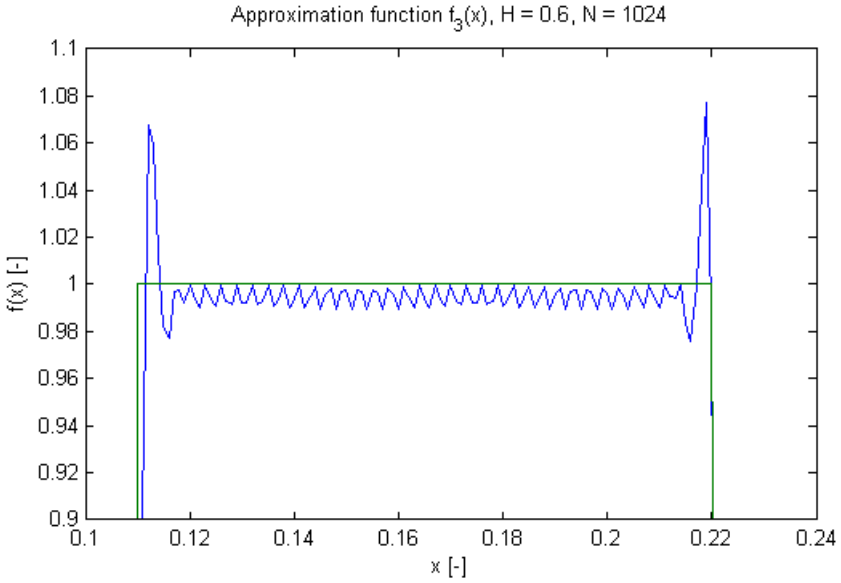

Figure 3.13: Gibb's effect of function $\bar{f}_3(x)$, $N = 1024$

3.1.2 Deformation Analysis

This section provides information about one dimensional rod analysis using BPM. One dimensional problem is principally based on function approximation that is described in Section 3.1.1. Thus the basic illustration of this method is only shown.

Following Figures 3.14, 3.15 and 3.16 show deformation with various stiffness $E(x)$. All those graphs were discretized using 64 nodes at interval $\langle -1, 2\rangle$, $p = 5$ and the parameter H was set to optimal value. Similarly to the problem of function approximation, the Gibb's effect can be observed at those figures, especially in Figure 3.14 at values $x = -1$, $x = 0$, $x = 1$ and $x = 2$ corresponding to the points of discontinuity.. The deformation outside that interval is equal to zero due to discretization of $\varphi(x)$ deformation just on this interval.

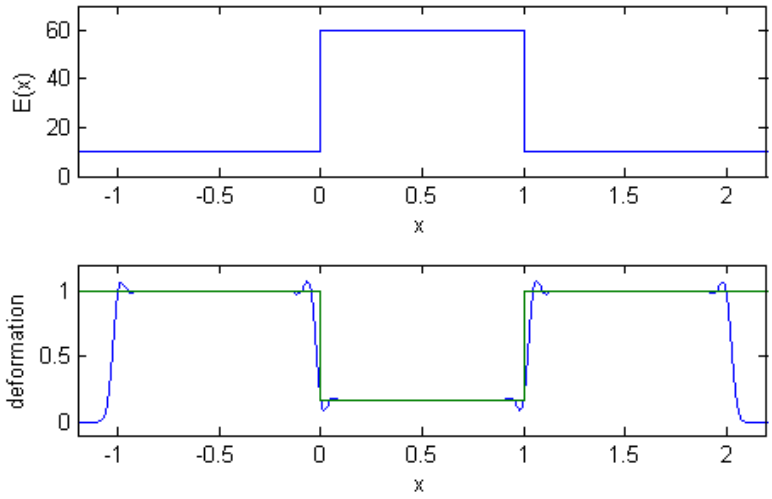

Figure 3.14: Graph of stiffness $E(x)$ and deformation $\varepsilon(x)$, $N = 64$, $p = 5$, $H = 0.7$

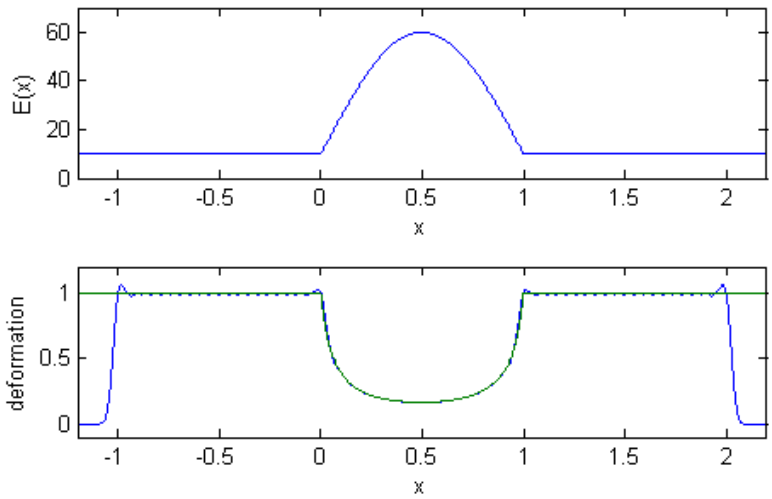

Figure 3.15: Graph of stiffness $E(x)$ and deformation $\varepsilon(x)$, $N = 64$, $p = 5$, $H = 0.6$

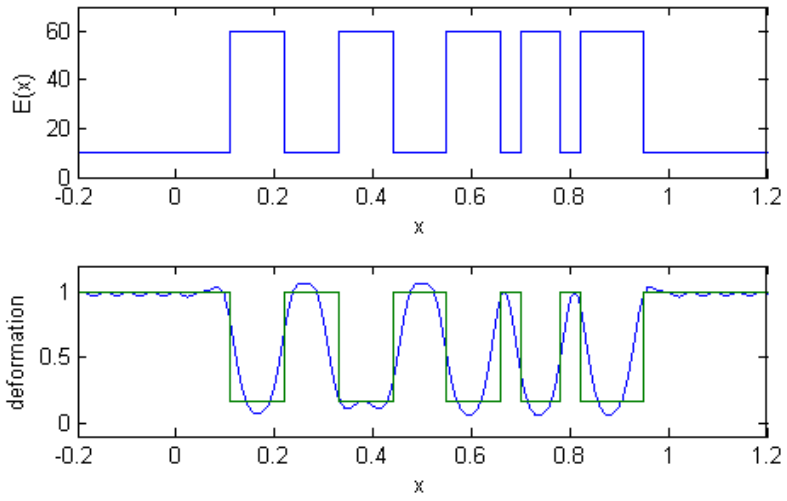

Figure 3.16: Graph of stiffness $E(x)$ and deformation $\varepsilon(x)$, $N = 64$, $p = 5$, $H = 0.5$

It can be noticed that deformation shown in Figure 3.16 does not provide sufficient accuracy, hence the surveyed interval was discretized using 256 nodes leading to strain profiles shown in Figure 3.17.

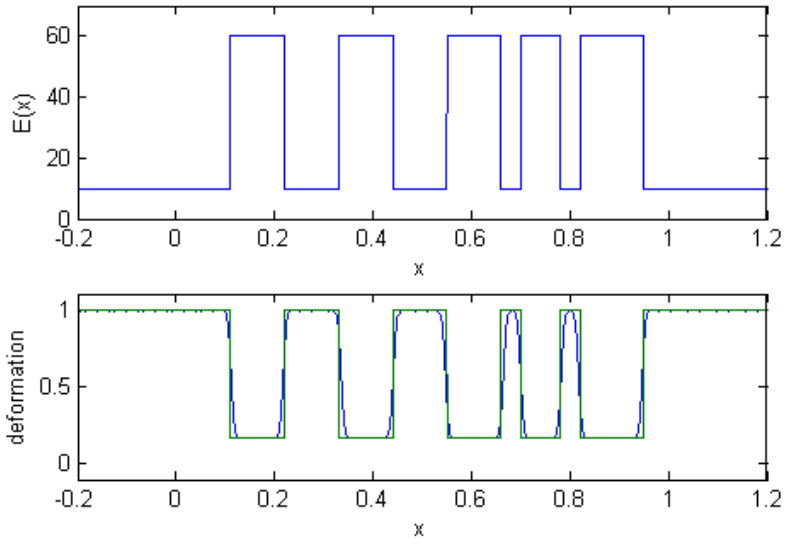

Figure 3.17: Graph of stiffness $E(x)$ and deformation $\varepsilon(x)$, $N = 256$, $p = 5$, $H = 0.6$

Finally, the BPM method was tested with parameter $p = 100$ that is provided in Figure 3.18. In comparison with previous Figure 3.17 it can be concluded that the parameter p does not influence a deformation distribution.

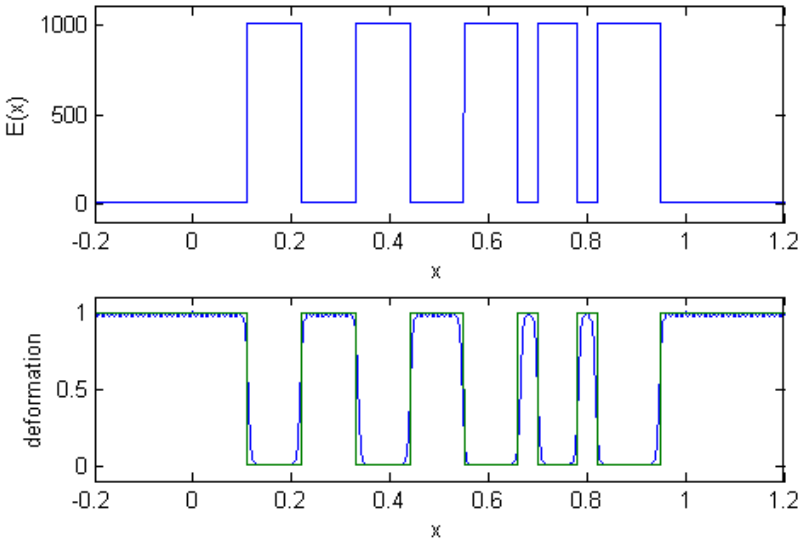

Figure 3.18: Graph of stiffness $E(x)$ and deformation $\varepsilon(x)$, $N = 256$, $p = 100$, $H = 0.6$

3.2 Fast Fourier Transform Based Method

This section provides information about Fast Fourier Transform Based Method. This method is based on analysing the medium that is made from periodically repeating cell as stated previously in Section 1.3. The cell is unambiguously described with the stiffness function $E(x)$ at interval $\langle a, b)$. Without the loss of generality we can assume that the interval is $\langle 0, 1)$. This section will provide information about this method using the particular basic cell with its p parameter along that interval.

First, we can take a look at the situation when we increase in number of nodes while the rest of parameters is kept constant. This condition is met in Figure 3.19 that provides information about number of iterations with regard to number of nodes. The graph is almost constant (the same trend can be observed for various inputs of E_1 stiffness) thus it means that the number of iteration does not depend on the number of nodes involved. Hence the number of nodes just increases the deformation accuracy of the medium that is analysed.

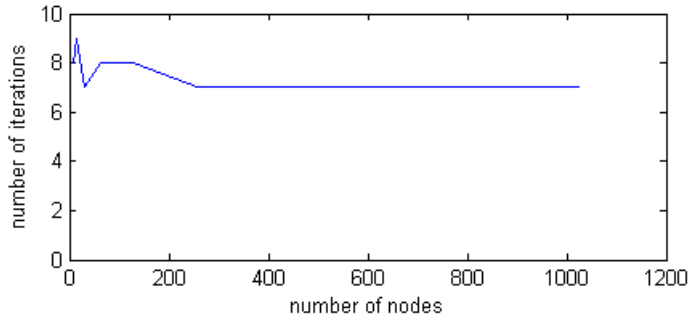

Figure 3.19: Number of iterations vs. number of nodes

Next we can provide some information about the parameter symbolised as E_{ref}. This parameter is very important for the convergence of the method. The unsuitable value can cause the slow rate of convergence and so the inefficiency of the method or even divergence

of the method.

Figure 3.20 shows graphs where the number of iterations versus the value $\frac{E_{ref}}{E_0}$ is shown for different ratio $p_{max} = \frac{E_1}{E_0}$. It is necessary to note that all of the graphs were calculate for particular value of nodes $N = 1024$. We can notice that the values of E_{ref} that are close to E_0 stiffness cause the inefficiency or even divergence of the method. An increase in E_{ref} parameter leads to very fast convergence. The optimal behaviour is observed somewhere between E_0 and E_1 stiffness. Finally, the next increase in E_{ref} over E_1 leads to the growth in number of iteration thus the method becomes ineffective again.

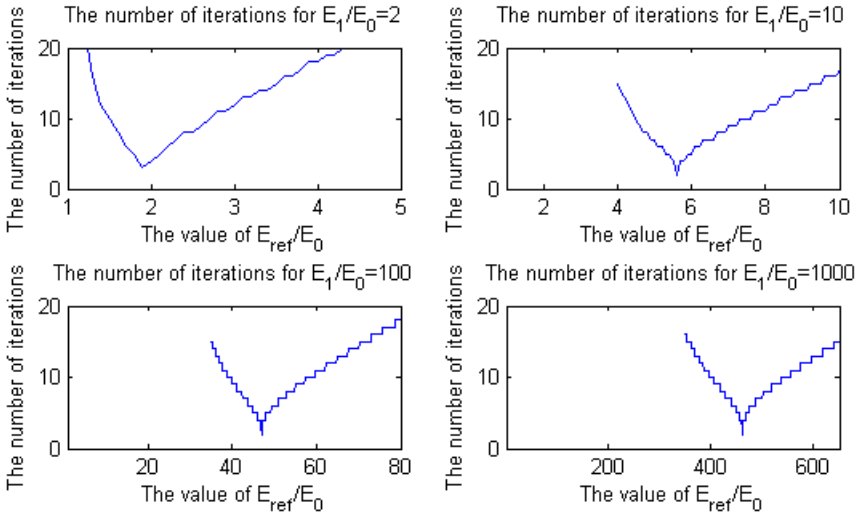

Figure 3.20: The number of iterations vs the value of E_{ref}/E_0

Next we are going to show information about the value of E_{ref} parameter in relation to E_0 and E_1 stiffness. It is shown in Figure 3.21 where the vertical axis provides values of $(E_{ref} - E_0)/(E_1 - E_0)$ meaning that the value 0 represents E_0 stiffness and the value 1 represents E_1 stiffness. The best fit value E_{ref} is plot against the p_{max} ratio. In order to get a better readable graph the horizontal axis is log scaled. The exact values for graph generation are provided in Table 3.2.

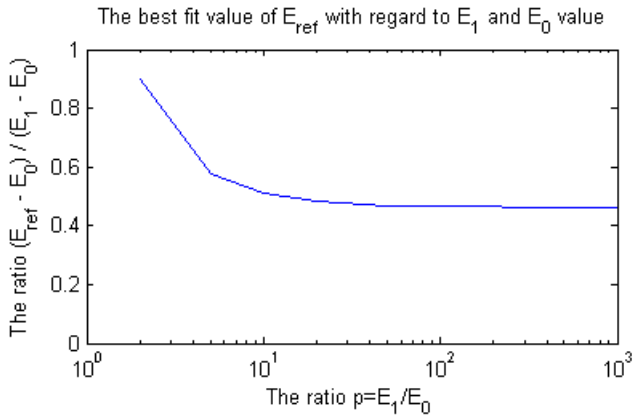

Figure 3.21: Best fit value of E_{ref} versus the p_{max} ratio

$p = E_1/E_0$	2	5	10	20	50	100	500	1000
$(E_{ref} - E_0)/(E_1 - E_0)$	0.900	0.575	0.511	0.484	0.469	0.465	0.4609	0.4605

Table 3.2: The determination of E_{ref} with regard to E_1 and E_0 value

Finally Figure 3.22 shows overall solution using 1024 nodes and concrete values that are following: $E_0 = 10$, $p_{max} = 5$ and the basic cell is set on interval $\langle 0, 1)$ as usual. The top left graph shows both E_0 and E_1 stiffness of the medium. The top right graph shows the ε_1 deformation. The bottom left graph provide information about stress along the basic cell. The small deviation from constant function can be suppressed by increasing in the number of iterations.

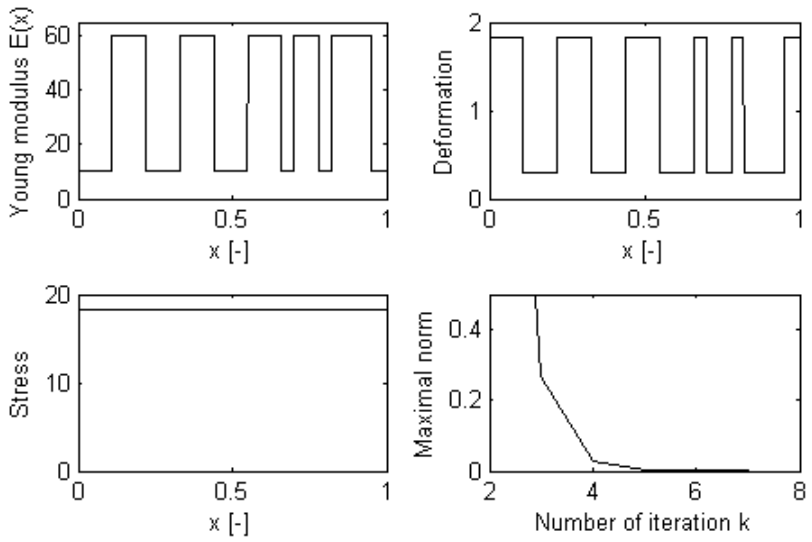

Figure 3.22: Overall solution using 1024 nodes

3.3 Conclusion

Primarily, this section provides a summary of the methods involved and subsequently the brief discussion on future work.

The analysing of one dimensional rod using Boundary Point Method is mostly based on accuracy of function approximation with basis function

$$\varphi(x) = \frac{1}{\sqrt{\pi H}} e^{-\frac{|x|^2}{Hh^2}}$$

.

The most important for approximation is H parameter and the number N of discretizing nodes. The information about the method can be summarized into following items:

- the increase in the discretizing nodes N leads to a better approximation
- the optimal value of H is rather complicated, the setting of this parameter mostly depends on function properties, especially its continuity
- for observed functions, the optimal value of H parameter using ℓ^2 norm lies in interval $\langle 0.4, 3.3 \rangle$, the fast varying functions have smaller optimal value of H parameter
- maximal norm is not suitable for discontinuous functions
- the main problem of approximation is called Gibb's effect causing oscillation of approximated functions at the points of discontinuity

The Fast Fourier Transform-Based Method convergence is mainly based on the E_{ref} value and the number of discretizing nodes N and the results about them are summarized in following items:

- the increase in the discretizing nodes N does not influence the number of iterations, it just specifies the observed interval while the iterations is kept the same
- the optimal value of E_{ref} lies between E_0 and $(E_0 + E_1)$ value; for the close values of matrix and heterogeneity stiffness, the optimal E_{ref} lies close to $(E_0 + E_1)$ stiffness; for the ratio $\frac{E_0+E_1}{E_0}$ greater than approximately 5, the optimal value of E_{ref} is close to value $\left(E_0 + \frac{E_1}{2}\right)$

Future work dealing with these methods could be focused on following problems:

- the Gibb's effect caused by function approximation in BPM could be explored and possibly diminished
- the analytical solution of one dimensional problem using FFT-Based Method could be obtained
- the methods could be expanded into two dimensional or even into three dimensional spaces
- the speed of calculation of both methods should be investigated and consequently improved

Bibliography

[1] Finite element method tutorial [online].

[2] Novák J. One dimensional elastic infinite composite media discretized by boundary point method explored from the convergence point of view, 2007.

[3] Suquet P. Michel J.C., Moulinec H. Effective properties of composite materials with periodic microstructure: a computational approach. *Computer methods in applied mechanics and engineering*, 1998.

[4] Wikipedia. Dirac delta function [online], 2008.